MOLECULAR AND CELLULAR BIOLOGY, Feb. 1987, p. 830–837
0270-7306/87/020830-08$02.00/0

Vol. 7, No. 2

Expression of H-*ras* Correlates with Metastatic Potential: Evidence for Direct Regulation of the Metastatic Phenotype in 10T1/2 and NIH 3T3 Cells

SEAN E. EGAN,[1] GRANT A. McCLARTY,[1] LENKA JAROLIM,[1] JIM A. WRIGHT,[1] IRA SPIRO,[2] GORDON HAGER,[3] AND ARNOLD H. GREENBERG[1]*

The Manitoba Institute of Cell Biology, University of Manitoba, Winnipeg, Manitoba, Canada R3E 0V9[1]; Division of Radiation Oncology, George Washington University, Washington, D.C. 20037[2]; and Laboratory of Tumor Virus Genetics, National Cancer Institute, Bethesda, Maryland 20205[3]

Received 25 July 1986/Accepted 19 November 1986

Using three independent approaches, we studied the effects of H-*ras* on metastasis formation. Analysis of five in vitro-*ras*-transfected 10T1/2 clones with either flat or refractile morphologies revealed a relationship between metastatic potential, H-*ras* expression, and anchorage-independent growth. Four metastatic variants derived from a poorly metastatic, low-H-*ras*-expressing line all expressed high levels of H-*ras* RNA and grew efficiently in soft agar. Activation of H-*ras* expression in the metastatic tumors had occurred through amplification and rearrangement of H-*ras* sequences. In addition, preinduction of p21 synthesis in NIH 3T3 line 433, which contains v-H-*ras* under transcriptional control of the glucocorticoid-sensitive mouse mammary tumor virus long terminal repeat, significantly increased metastatic efficiency. Glucocorticoid treatment of normal or pEJ-transformed NIH 3T3 cells did not affect metastatic potential. These data reveal a direct relationship between *ras* expression and metastasis formation and suggest that metastatic and transformed phenotypes may be coregulated in *ras*-transformed 10T1/2 and NIH 3T3 cells.

Tumor progression is the tendency of tumors to become more aggressive with time. The widely accepted model is that described originally by Foulds (11), in which progression was characterized by emergence of new variants with a selective advantage for growth in the host. Metastatic spread is the most important form of tumor progression because it is the most life-threatening aspect of the disease. Metastasis is a complex process involving invasion through host barriers into the vasculature and survival against circulating host immune defenses, followed by implantation, extravasation, and growth at sites distant to the primary neoplasm (24, 25, 27, 34).

Much effort has been directed at understanding the metastatic cascade, yet little is known about the mechanisms involved. On the other hand, the critical events in cell immortalization and transformation have been partially elucidated and attributed to mutation or disregulation of a group of genes collectively known as oncogenes. These genes are normally responsible for maintenance of control over diverse cellular functions including proliferation, differentiation, morphological regulation, communication, and motility (3, 20, 22, 33, 40). Consequently, they are good candidates for study of the metastatic process, which also requires alterations of many of these functions (24, 27, 34).

Recent studies showed that primary and established rodent fibroblasts transformed by activated *ras* sequences can form metastases (12, 18, 23, 27, 36). Exclusive selection and analysis of in vitro-transformed foci, however, raises the possibility that *ras* transformation may be a permissive event for expression of the metastatic phenotype but may not be directly involved. To resolve this question we analyzed the relationship between *ras* expression and metastatic potential. *ras*-mediated transformation may be the initial event which allows expression of secondary cellular characteristics important in metastatic conversion, or it may be more directly involved in maintaining and regulating the metastatic phenotype through expression and action of its gene product. Recent work demonstrated a relationship between levels of H-*ras* oncogene (21, 42) or proto-oncogene (29) expression and tumorigenic potential. In addition, it has been shown that morphological reversion of the *ras*-transformed phenotype may be achieved through microinjection of anti-p21 antibodies (8). Consequently, *ras* expression is critical in maintaining the transformed phenotype. In this report we provide evidence for the direct involvement of *ras* expression in metastatic potential, suggesting that *ras*-mediated tumorigenic and metastatic phenotypes may be regulated through a common mechanism in both 10T1/2 and NIH 3T3 cells.

MATERIALS AND METHODS

Gene transfer, plasmids, and in vitro-derived cell lines. DNA-mediated gene transfer or transfection was performed by using the calcium phosphate method as previously described (41). Plasmid pAL8A was constructed by introducing the 6.6-kilobase (kb) T24 H-*ras* insert into the *Bam*HI site of pSV2neo. After transfection of pAL8A into 10T1/2 cells, three morphologically transformed cell lines were established and cloned from foci observed at confluence. These cell lines, designated CIRAS-1, -2, and -3, were subsequently shown to be resistant to 400 μg of G418 sulfate (GIBCO Laboratories, Grand Island, N.Y.) per ml. Two other cell lines were isolated by selection in 400 μg of G418 per ml. These two lines, NR3 and NR4, were morphologically nontransformed. Focus formation was observed at a frequency of 2×10^{-4} per cell per μg of DNA. In contrast,

* Corresponding author.

after G418 selection, the frequency of resistance was 4×10^{-4} per cell per μg of DNA, which resulted in 60% flat and 40% refractile colonies. MDS.R cell lines are radiation-transformed 10T1/2 cells which were selected for anchorage-independent growth and tumorigenicity (30). All 10T1/2-derived cell lines were grown in either αMEM or F12 medium (Flow Laboratories, Inc., McLean, Va.) supplemented with 10% fetal calf serum (GIBCO).

NIH 3T3 line 433, which contains v-H-*ras* under the control of the glucocorticoid-sensitive mouse mammary tumor virus long terminal repeat (plasmid pA9) (13), was grown in αMEM (GIBCO) and 10% fetal calf serum with or without 2×10^{-6} M dexamethasone (Sigma Chemical Co., St. Louis, Mo.) for 7 days before injection into BALB/c *nu/nu* mice. Growth with dexamethasone under these conditions results in a 20-fold increase in p21 synthesis (13). Control cell lines pEJ1 and pEJ3 were obtained by transfection of pEJ H-*ras* into NIH 3T3 cells and cloned by limiting dilution from transformed foci. NIH 3T3-derived cell lines were maintained in αMEM media supplemented with 10% calf serum (Colorado Serum Co., Denver, Colo.). All cells were kept in culture for a maximum of approximately 2 months, after which they were discarded and replaced by frozen stocks to minimize drift from the original clones.

Experimental and spontaneous metastasis assays. Metastatic potential was determined by the experimental metastasis assay with a tumor cell inoculum of 3×10^5 (except with NIH 3T3 line 433, for which 5×10^5 cells were used) injected in a 0.2-ml volume into the tail vein of mice (9). Cells were lightly trypsinized from subconfluent cultures, washed, and adjusted to the appropriate concentration in Hanks balanced salt solution. Recipient animals were sacrificed 21 days later by ether anesthesia and Bouin solution (picric acid, formaldehyde, acetic acid [15:5:1]) injected intratracheally. The stained lungs were then removed, and metastatic foci were counted under a dissecting microscope.

Spontaneous lung metastasis formation was assayed between 30 and 60 days after subcutaneous injection. Lung metastases were occasionally visible but were normally detected as micrometastases by culturing enzymatically disaggregated lung cells in 400 μg of G418 per ml (see below).

In vivo-derived cell lines. In vivo-derived cell lines were obtained by dissecting out the tumor, cutting and teasing it into small fragments, and enzymatically disaggregating it (800 μg of collagenase type I [Sigma] per ml, 10 U of hyaluronidase type I-S [Sigma] per ml, 0.05% trypsin-EDTA [GIBCO]), followed by selection of plasmid-carrying cells in 400 μg of G418 sulfate per ml for 3 days. NR3.1L lines were derived from two C3H/HeN mice with rare experimental lung metastases after intravenous injection of 10^6 NR3 cells. NR3.3 and NR3.4 lines were isolated from nonregressing tumors 40 to 45 days after subcutaneous injection of 3×10^5 NR3 cells into C3H/HeN mice.

Growth in semisolid medium. Growth in soft agar was performed basically as previously described (36) with a 0.5% Bacto-Agar (Difco Laboratories, Detroit, Mich.)–10% fetal calf serum–αMEM base layer and a 0.33% agar–10% fetal calf serum–αMEM growth layer. Colonies were scored after 14 days.

Northern and Southern blot analysis. Total RNA was prepared by the guanidinium-cesium chloride method previously described (4), and 20 μg was electrophoresed on 1% formaldehyde gels (16). The RNA was then transferred to nitrocellulose and hybridized at 68°C for 16 h to a ^{32}P-labeled (3×10^8 cpm/μg) nick-translated (32) v-H-*ras* probe (Oncor Inc., Gaithersburg, Md.). The filters were washed in 2× SSC (1× SSC is 0.15 M NaCl plus 0.015 M sodium citrate)–0.1% sodium dodecyl sulfate (SDS) (twice for 15 min each at room temperature) followed by 0.1× SSC–0.1% SDS (once for 30 min at room temperature and once for 30 min at 65°C). Autoradiography was performed at −70°C with X-Omat AR film (Eastman Kodak Co., Rochester, N.Y.) and Cronex lighting plus intensifying screens. Total RNA (20 μg) was also electrophoresed on 0.6% agarose gels in TBE buffer (0.089 M Tris borate, 0.089 M boric acid, 0.002 M EDTA) (19, 37) and stained with ethidium bromide to confirm relative quantitation and ensure that degradation had not occurred.

Southern blot analysis was performed with two different protocols using *Bam*HI and *Eco*RI. When *Bam*HI was used, 20 μg of genomic DNA was digested and separated on a 0.6% agarose gel, transferred to a nylon membrane (Bio-Rad Laboratories, Richmond, Calif.) with 0.4 N NaOH, and hybridized for 24 h to a ^{32}P-labeled (Klenow extension [7]; 3×10^8 cpm/μg) v-H-*ras* probe (50% formamide at 42°C), as previously described (31). Alternatively, 20 μg of genomic DNA was digested with *Eco*RI and electrophoresed on a 0.45% agarose gel. The DNA was then transferred to nitrocellulose (35) and hybridized at 42°C (50% formamide, 10% dextran sulfate) for 16 h to a ^{32}P-labeled (nick translated [32]; 3×10^8 cpm/μg) v-H-*ras* probe. After hybridization, filters were washed in 2× SSC–1.0% SDS (twice for 15 min each at room temperature) and 0.1× SSC–0.1% SDS (twice for 30 min each at 65°C).

Densitometric analysis. Relative levels of H-*ras* mRNA were determined by densitometry with the Bio-Rad Model 165D Transmittance/Reflectance Scanning Desitometer. Peaks were cut and weighed, and ratios were determined from three Northern blots. Reprobing with β-tubulin or c-*myc* revealed that differences in *ras* RNA were not a result of differential loading of mRNA (results not shown).

RESULTS

Metastatic potential of in vitro-derived cell lines. Transfection of pAL8A into 10T1/2 cells allowed us to introduce T24 H-*ras* linked to a selectable (neomycin resistance) marker gene. Five clones were picked and expanded for analysis. Three transformed foci gave rise to the cell lines CIRAS-1, -2, and -3, whereas cell lines NR3 and NR4 arose from flat colonies selected in G418. CIRAS-1, -2, and -3 cells were disorganized and consistently overlapped; NR3 cells were flat, contact inhibited, and organized (similar to 10T1/2); and NR4 cells were intermediate for these characteristics (Fig. 1). The isolation of cell lines with different colony morphologies ultimately enabled us to analyze the relationship between *ras* expression and various phenotypic properties, including tumorigenic and metastatic potentials.

Survival and tumor latency data (Table 1) indicate that CIRAS-2 and -3 were the most tumorigenic of the five lines, CIRAS-1 and NR4 showed intermediate tumor latency, and NR3 was poorly tumorigenic, with many of the tumors regressing. Subcutaneous injection of up to 10^7 control 10T1/2 cells into either syngeneic C3H/HeN or immunodeficient BALB/c *nu/nu* mice did not result in tumor formation.

Spontaneous metastases were detected in all mice injected with CIRAS-1, -2, or -3, whereas three of five mice injected with NR4 and none of five injected with either NR3 or parental 10T1/2 developed tumors at other sites (Table 1). To quantitate metastatic potential, the lung colonization or

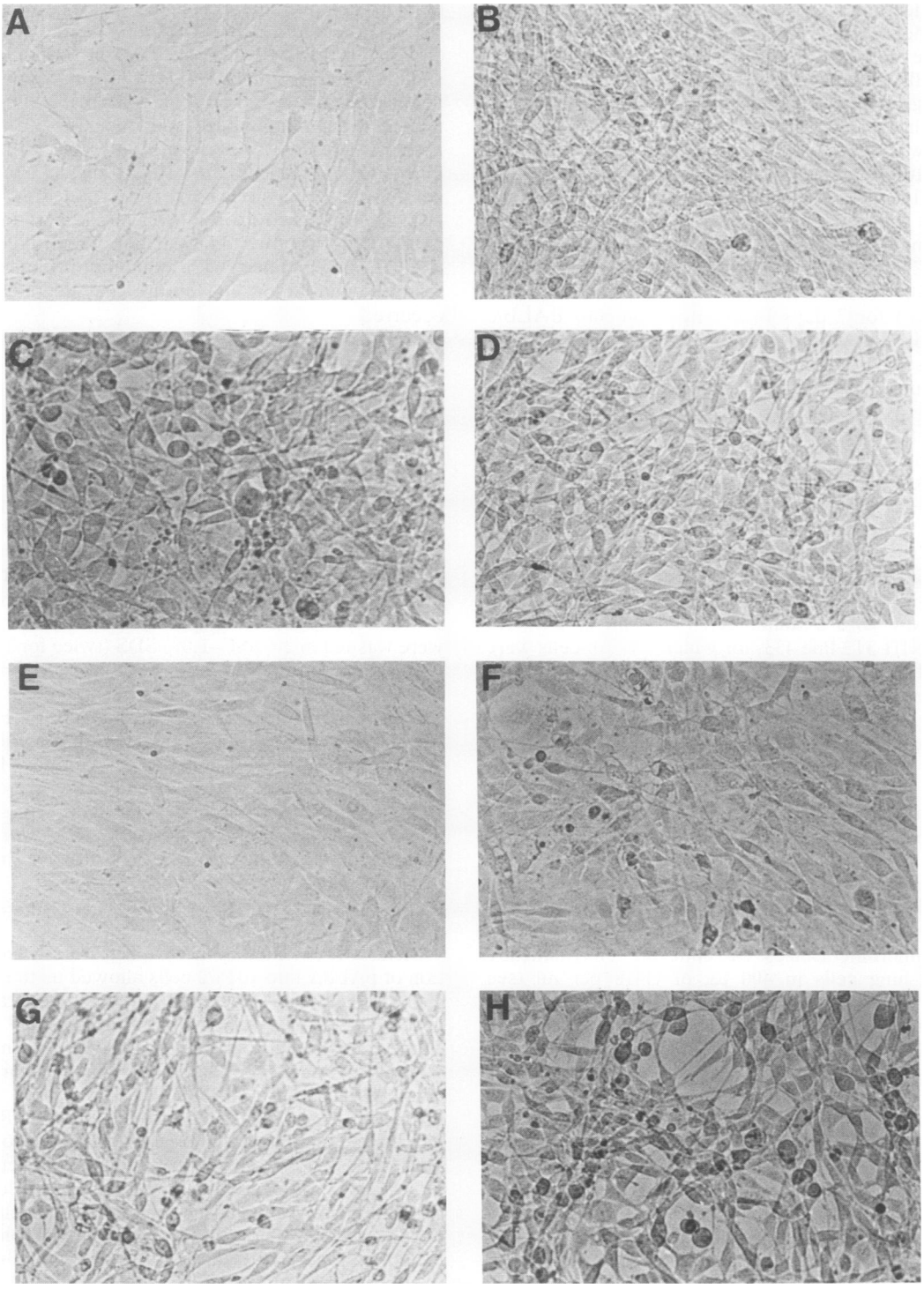

FIG. 1. Photomicrographs illustrating morphological differences between 10T1/2 cells (A) and T24-H-*ras*-transfected cell lines CIRAS-1 (B), CIRAS-2 (C), CIRAS-3 (D), NR3 (E), and NR4 (F) as well as in vivo-derived metastatic variants NR3.4 (G) and NR3.1LB (H).

experimental metastasis model was used. With this assay, CIRAS-2, and -3 were highly metastatic, CIRAS-1 and NR4 were relatively poorly metastatic, and NR3 was virtually nonmetastatic, with only 3 of 43 mice injected producing lung tumors and two of these producing tumors only at the highest cell inoculum (10^6). Control 10T1/2 cells transfected with pSV2neo produced only rare experimental metastases (one tumor each in two of six mice injected with 3×10^5 cells each). Radiation-transformed 10T1/2 cell lines (MDS.R) were tumorigenic but not metastatic (Table 1).

A correlation between anchorage-independent growth and metastatic potential has been observed in several systems (5, 36). We assessed the cloning efficiency in agar of all five transfected lines and the 10T1/2 control (Table 1). The

TABLE 1. Tumorigenic and metastatic characteristics of T24-H-*ras*-transformed 10T1/2 lines in syngeneic C3H/HeN mice

Cell line	Tumorigenicity[a]			Exptl metastases[b]		Frequency of spontaneous metastases[c]	Frequency (mean ± SE) of cloning in soft agar with tumor inoculum[d]			Division time (h)
	Frequency	Latency (days [mean ± SE])	Survival (days [mean ± SE])	Frequency	No. (mean ± SE)		10^3	10^4	10^5	
10T1/2	0/12			0/12	0	0/5	0 ± 0	0 ± 0	0 ± 0	14
CIRAS-1	13/13	10.0 ± 1.0	66.5 ± 7.0	20/27	14 ± 5	5/5	0 ± 0	0.6 ± 4	14 ± 2	14
CIRAS-2	11/11	6.5 ± 0.7	58.2 ± 9.5	8/8	118 ± 6	5/5	9 ± 2	360 ± 11	>500	9.7
CIRAS-3	11/11	6.5 ± 0.7	36.2 ± 4.2	14/14	121 ± 20	5/5	7 ± 1	296 ± 99	>500	12.3
NR4	10/10	10.7 ± 1.4	58.5 ± 12.4	12/19	2 ± 0.5	3/5	0 ± 0	1 ± 1	0.2 ± 0.2	14
NR3	6/8	49.6 ± 2.0	106.0 ± 7.0	1/13	0.1 ± 0.1	0/5	0 ± 0	0 ± 0	0 ± 0	15.3
MDS.R1	5/5	7.1 ± 0.9	NT[e]	0/3	0	0/5				
MDS.R5	5/5	8.1 ± 1.1	NT	0/6	0	0/5				
MDS.R9	5/5	8.7 ± 1.3	NT	0/3	0	0/5				
MDS.R25	5/5	4.0 ± 0	NT	0/4	0	0/5				

[a] Results are reported for subcutaneous injection of 3×10^5 cells. Survival data is taken from one experiment with four to eight mice per group. NR3 survival is based on three mice that developed nonregressing tumors, and latency is based on six mice with detectable tumors.
[b] Data were obtained after injection of 3×10^5 cells, except for MDS lines, which were injected as a 10^6 cell inoculum.
[c] Gross spontaneous metastases were occasionally seen; however, micrometastases detected by culturing lung cells in 400 μg of G418 per ml were detected for CIRAS-1, CIRAS-2, CIRAS-3, and NR4 tumors.
[d] Five replicate plates were used for each experimental point.
[e] NT, Not tested.

results correlated well with in vivo metastatic potential; CIRAS-2 and -3, the most metastatic lines, grew very efficiently in agar, whereas CIRAS-1 and NR4 grew very poorly and were inefficient at forming lung foci. NR3 rarely produced agar colonies (results not shown) or metastases. 10T1/2 never grew in soft agar.

Southern blotting revealed the presence of novel H-*ras* sequences in all five lines (Fig. 2); however, gene copy number did not correlate with in vivo behavior. Northern blot analysis was also performed, and 1.2-kb messages were detected in all lines (Fig. 3). In addition, CIRAS-1 also expressed high levels of a 4.7-kb species. Densitometric analysis of three Northern blots revealed a relationship between expression of H-*ras* and metastatic potential in immunocompetent C3H/HeN mice (Fig. 4a), as well as in natural-killer-cell-deficient C3H/HeJ *bg/bg* mice and their normal *bg/+* littermates (Fig. 4b). Consideration of the 4.7-kb species as a translatable message (6) yielded the relationship shown in Fig. 4a ($r = 0.899$). Inclusion of only the 1.2-kb species in the calculations yielded essentially the same result ($r = 0.844$).

In vivo selection of metastatic variants. We next isolated four cell lines from two mice bearing rare NR3-derived experimental lung metastases (NR3.1LA, NR3.1LB, NR3.1LC, and NR3.1LD). These four lines were cultured from two distinct lung colonies in each animal and therefore represent tumors arising from four independent cells or emboli in vivo. The lines were all morphologically transformed (NR3.1LB, Fig. 1). In addition, they were highly tumorigenic, metastatic (Table 2), and grew efficiently in soft agar (results not shown). Two lines were also isolated from mice bearing nonregressing tumors after subcutaneous injection of NR3 cells. These tumor lines (NR3.3 and NR3.4)

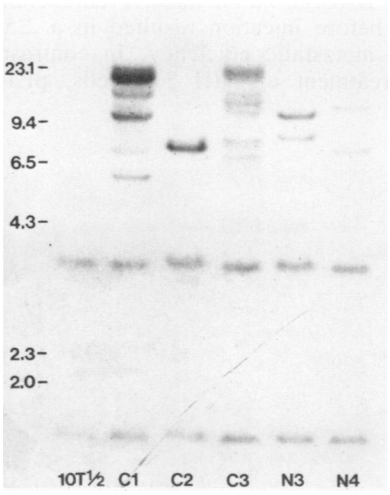

FIG. 2. Southern blot analysis of *Bam*HI-digested genomic DNA (20 μg), showing the presence of T24 H-*ras* sequences in transfectant lines. C1, CIRAS-1; C2, CIRAS-2; C3, CIRAS-3; N3, NR3; N4, NR4. The numbers on the left are kilobases.

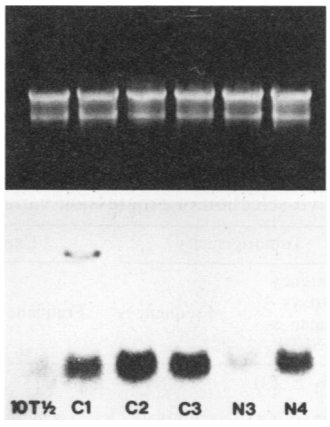

FIG. 3. Northern blot analysis of T24-H-*ras*-transfected cell lines (bottom panel). Transcripts of 1.2 and 4.7 kb were detected. The top panel shows ethidium bromide-stained nondenaturing gel with 20 μg of total RNA from each cell line, indicating equal loading for Northern blots. C1, CIRAS-1; C2, CIRAS-2; C3, CIRAS-3; N3, NR3; N4, NR4.

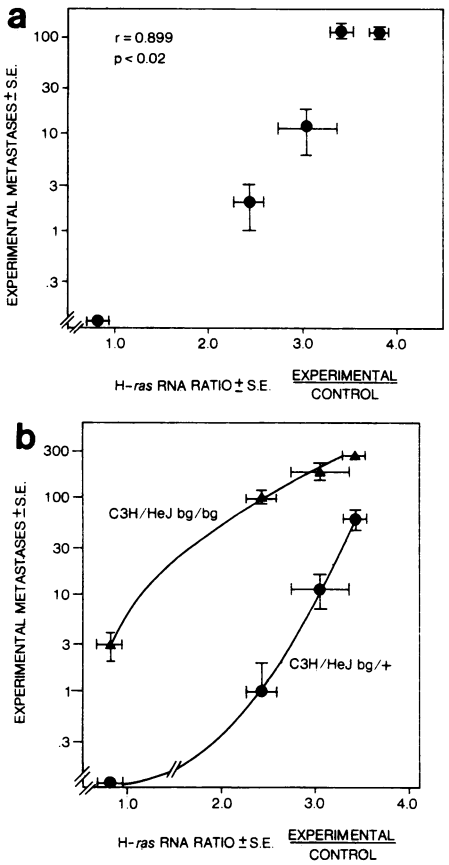

FIG. 4. Relationship between metastatic potential and H-*ras* expression assessed in (a) immunocompetent syngeneic C3H/HeN mice and (b) natural-killer-cell-deficient syngeneic C3H/HeJ *bg/bg* mice and normal heterozygous *bg/+* littermates. The Order of H-*ras* RNA ratios from lowest to highest were NR3, NR4, CIRAS-1, CIRAS-3, and CIRAS-2. CIRAS-2 was not tested in *bg/bg* mice. All RNA ratios were calculated by comparing *ras*-transfected lines to 10T1/2 controls.

were also refractile (Fig. 1), highly tumorigenic, and metastatic (Table 2).

All six in vivo-derived cell lines expressed high levels of H-*ras* RNA compared with the poorly expressing NR3 parental line from which they arose (Fig. 5). Evidence that gene rearrangement and amplification had occurred in the lung metastases (NR3.1L) was found on Southern blots (Fig. 6). All four metastatic lines showed complex and identical

TABLE 2. In vivo selection of progression variants of NR3 line

Cell line	Tumorigenicity		Exptl metastases	
	Latency (days [mean ± SE])	Frequency	Frequency	No. (mean ± SE)
NR3	49.6 ± 2.0	6/8	1/13	0.1 ± 0.1
NR3.1LA	6.8 ± 0.5	5/5	6/6	49 ± 7
NR3.1LB	9.8 ± 1.5	5/5	6/6	40 ± 18
NR3.1LC	6.7 ± 0.7	5/5	6/6	30 ± 6
NR3.1LD	5.8 ± 0.6	5/5	6/6	13 ± 7
NR3.3	9.8 ± 0.5	5/5	4/4	16 ± 5
NR3.4	13.8 ± 2.2	5/5	4/4	42 ± 19

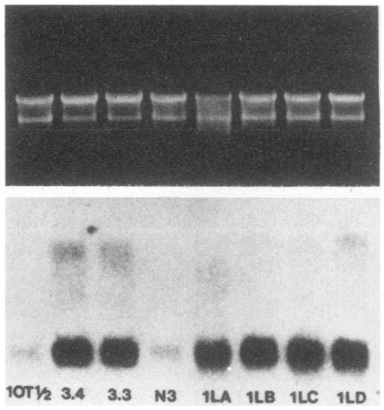

FIG. 5. Northern blot analysis of H-*ras* RNA levels in NR3-derived subcutaneous tumor lines (NR3.4 [3.4] and NR3.3 [3.3]), NR3-derived lung metastases lines (NR3.1LA [1LA], NR3.1LB [1LB], NR3.1LC [1LC], and NR3.1LD [1LD]), with NR3 (N3) and 10T1/2 controls. The top panel shows ethidium bromide-stained nondenaturing gel with 20 μg of total RNA from each cell line, indicating equal loading for Northern blots.

restriction patterns with novel H-*ras* sequences, indicating that they were of clonal origin. The subcutaneous tumors NR3.3 and NR3.4 were activated through gene rearrangement, resulting in only a single novel H-*ras* sequence. NR3.3 and NR3.4 exhibited the same restriction band, again indicating common origin. Southern blot analysis of these lines after BamHI digestion (results not shown) confirmed the identity of restriction patterns among all four metastatic lines and, independently, between the two subcutaneous tumors.

Induction of v-H-*ras* in NIH 3T3 cells. The relationship between activated H-*ras* expression and metastatic potential was then confirmed in the NIH 3T3 system by using line 433. Line 433 contains a plasmid (pA9) in which v-H-*ras* is transcriptionally regulated by the glucocorticoid-sensitive mouse mammary tumor virus long terminal repeat. It is able to enhance p21 production 20-fold in the presence of physiological amounts of glucocorticoids, resulting in a phenotype switch (13). After incubation in the presence or absence of dexamethasone for 7 days, line 433 was injected intravenously into BALB/c *nu/nu* mice. Preinduction of v-H-*ras* expression before injection resulted in a 2.5- to 3.0-fold increase in metastatic efficiency. In contrast, dexamethasone pretreatment of NIH 3T3 cells, pEJ-H-*ras*-trans-

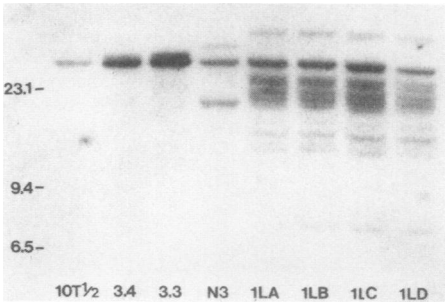

FIG. 6. Southern blot analysis of *Eco*RI-digested genomic DNA (20 μg) from NR3 (N3)-derived subcutaneous tumor lines (NR3.4 [3.4] and NR3.3 [3.3]) and lung metastasis lines (NR3.1LA [1LA], NR3.1LB [1LB], NR3.1LC [1LC], and NR3.1LD [1LD]). The numbers on the left are kilobases.

TABLE 3. Lung colony formation after p21 induction in line 433

Tumor line	Transfected gene	Dexamethasone treatment[a]	No. of lung metastases (mean ± SE[2]) (*n*)
433	MMTV LTR[b]/v-H-*ras*	−	70 ± 12 (7)
		+	181 ± 13[c] (9)
pEJ	pEJ H-*ras*	−	148 ± 40 (7)
		+	141 ± 40 (8)
CIRAS-1	T24 H-*ras*	−	3 ± 1 (7)
		+	4 ± 1 (9)
NIH 3T3		−	0.4 ± 0.2 (5)
		+	0.6 ± 0.6 (5)

[a] 2×10^{-6} M.
[b] MMTV LTR, Mouse mammary tumor virus long terminal repeat.
[c] $P < 0.001$.

formed NIH 3T3 cells, or T24-H-*ras*-transformed 10T1/2 controls did not affect their metastatic potential (Table 3).

DISCUSSION

We studied the effects of activated H-*ras* on metastatic potential in both 10T1/2 and NIH 3T3 cells and report that metastatic efficiency was closely related to the level of H-*ras* expression. H-*ras* RNA levels correlated with the tumorigenicity, anchorage-independent growth, and metastatic potential of a series of T24-H-*ras*-transfected 10T1/2 cell lines. Metastatic potential was assessed initially by the frequency of spontaneous metastases and quantitated with the experimental metastasis assay. This assay involves survival in the circulation, implantation, extravasation, and growth and has been found to correlate very well with spontaneous metastasis formation (14, 25). Although metastasis formation after intravenous injection does not require invasion through host barriers, this process may be quite similar to the extravasation process which is required for successful lung colonization.

The relationship between *ras* expression and metastatic efficiency was observed in immunocompetent (Fig. 4a) and natural-killer-cell-deficient *bg/bg* (Fig. 4b) mice, as well as in T-cell-deficient BALB/c *nu/nu* mice (A. H. Greenberg, S. E. Egan, L. Jarolim, and J. A. Wright, submitted for publication). The higher frequency of tumors in the *bg/bg* mice suggests that natural killer cells can reduce metastatic burden but do not affect relative metastatic efficiency (Greenberg et al., submitted). In vitro experiments also indicated that these cell lines were not sensitive to macrophage kill (results not shown). Furthermore, flow cytometric analysis has revealed that expression of MHC class 1 antigens on these lines is unaffected by *ras* transfection (B. Elliot and A. H. Greenberg, unpublished data). Consequently, it is unlikely that immune regulation is responsible for the relative metastatic efficiencies observed. It should also be noted that the tumorigenicity and anchorage-independent growth potential of these lines followed the same relationship, suggesting that *ras* expression may affect all three properties directly and through a common mechanism.

Radiation-transformed 10T1/2 lines (MDS.R) were found to be tumorigenic but nonmetastatic, indicating that tumorigenic transformation of 10T1/2 is insufficient for expression of the metastatic phenotype. In contrast, pSV2neo-transfected 10T1/2 controls produced occasional lung metastases, indicating that *ras* transformation is not the only mechanism by which metastatic cells may be generated. This is not unexpected since activated *ras* sequences can be detected in only a minority of human tumors (15). The mechanism by which these 10T1/2 *neo* cells acquired metastatic ability is unknown. Possibly, integration of transfected plasmid and carrier DNA was responsible for activation of local genes regulating the metastatic phenotype.

The six in vivo-derived NR3 lines were all highly tumorigenic, metastatic, and expressed high levels of H-*ras* RNA, indicating that selection of metastatic cells also resulted in selection for high H-*ras* expression. The existence of common restriction banding patterns on Southern blots (Fig. 2b) suggests that the four NR3.1L lines likely arose from the same cell, whereas the two subcutaneous tumor lines were derived from a different but common variant. Activation of H-*ras* expression may have occurred within the in vitro NR3 population, giving rise to preexisting high-H-*ras*-expressing subpopulations that preferentially formed lung tumors on inoculation. Derivation of lung metastases and subcutaneous lines in these experiments was performed by using parallel NR3 cultures of different passage numbers. Consequently, the selection of two distinct subpopulations (at subcutaneous and lung sites) was likely a result of the presence of different variants in these NR3 inocula. The existence of such variants in the NR3 population has been confirmed through in vitro selection of anchorage-independent or focus-forming metastatic subclones (M.-C. Gingras and A. H. Greenberg, unpublished results). Alternatively, it is possible that selection for subcutaneous tumor growth or metastatic ability resulted in the outgrowth of different phenotypic variants from an NR3 population containing both subpopulations. This explanation seems less likely since NR3.1L lines were selected for lung colonization but were tumorigenic at subcutaneous sites and NR3 tumor lines (NR3.3 and NR3.4) were selected for subcutaneous growth yet are metastatic.

The relationship between *ras* expression and metastatic potential was also evident in the NIH 3T3 system with line 433, which contains v-H-*ras* under transcriptional control of the glucocorticoid-sensitive mouse mammary tumor virus long terminal repeat. Induction of v-H-*ras* p21 synthesis before intravenous injection resulted in a significant increase in metastatic potential. Physiological glucocorticoids presumably induced v-H-*ras* in vivo (13) and could have been responsible for metastases from cells not incubated in dexamethasone before injection. Although both lines would express v-H-*ras* in vivo, in vitro induction likely provided a kinetic advantage that allowed more cells to survive and form lung tumors. This result also suggests that activated *ras* expression is important in the early events after intravenous injection (implantation and extravasation). Control experiments revealed that dexamethasone treatment did not potentiate the metastatic efficiency of lines constitutively expressing H-*ras*.

Greig et al. (12) recently reported that NIH 3T3 cells are both tumorigenic and metastatic under specific conditions. Their work suggests that transformation of NIH 3T3 cells by activated H-*ras* may enhance a preexisting metastatic phenotype. Their results emphasize the necessity for caution when interpreting the malignant characteristics of NIH 3T3-derived transformants. Although transfection of activated *ras* can enhance the metastatic potential of a preexisting malignant phenotype (39), it has been shown that *ras* expression in NIH 3T3 cells results in enhanced secretion of collagenase IV activity, as well as impartation of the ability

to invade amnion basement membranes on these cells (38). These properties are not shared by NIH 3T3 cells or spontaneous transformants (38). In addition, induction of the metastatic phenotype by activated *ras* does not require aneuploid recipient cells such as NIH 3T3 but has been observed in diploid fibroblasts (23, 28). Consequently, *ras* transformation can result in metastatic conversion in some cell systems. Previous studies did not determine whether this phenomenon is a direct result of *ras* expression or whether *ras* transformation may only be permissive for expression of secondary events which then lead to appearance of the metastatic phenotype. Our studies were undertaken to evaluate the relative importance of these two possible roles for *ras* in metastasis formation. We confirmed previous work and report that 10T1/2 cells were also susceptible to *ras*-mediated metastatic conversion. More relevant to the hypothesis that *ras* directly affects the expression of the metastatic phenotype, a correlation between *ras* expression and metastatic potential was demonstrated: (i) the metastatic potential, tumorigenicity, and anchorage-independent growth properties of five *ras*-transfected lines all followed the same relationship and correlated with H-*ras* RNA expression, (ii) in vivo-derived metastatic variants exhibited high H-*ras* expression, and (iii) induction of the v-H-*ras* gene resulted in enhanced metastatic efficiency. This does not support integrational activation of "metastatic genes" as a mechanism of *ras*-mediated metastatic conversion. In particular, induction of *ras* expression in line 433 clearly affects expression of the metastatic phenotype, presumably without karyotypic changes. Although this study involved a limited number of *ras*-transfected cell lines, we believe that the three independent approaches taken together strongly support a tight link between *ras* action and the metastatic phenotype. This relationship has not been established at the protein level (*ras* p21); however, the correlation between the metastatic, tumorigenic, and anchorage-independent characteristics of these lines suggests that *ras* affects all three processes through a common mechanism. These results provide evidence for a direct role for activated *ras* in regulating and maintaining the metastatic phenotype.

In contrast to the results obtained in 10T1/2, NIH 3T3, and diploid fibroblasts, Mushel et al. (23) reported that *ras*-transformed C127 cells are not metastatic. Therefore, not all lines expressing activated *ras* sequences are converted to the metastatic phenotype. Indeed, infection of PC12 neuronal cells by *ras*-containing retroviruses induces them to differentiate (26). It has been suggested that *ras* p21 is important in signal transduction processes via secondary messengers (17), and evidence is accumulating that p21 might normally be involved in coupling of receptors for polypeptide agonists to phospholipase C (1, 10). Consequently, phenotypic alterations induced by *ras* would be cell-type dependent and likely influenced by genes that are transcriptionally active or that are capable of being induced as a result of p21 function. Identification and characterization of these metastatic genes or gene products which are induced or altered by *ras* may lead to a greater understanding of the process by which transformed cells evolve to the metastatic phenotype.

After submission of this manuscript, Bradley et al. (2) reported that various *ras* contructs were capable of converting NIH 3T3 to metastatic cells. In addition, this group described rapid acquisition of the metastatic phenotype without in vitro selection. These results are consistent with our findings, but the effect of *ras* expression on metastatic potential reported here supports direct regulation of the metastatic phenotype as opposed to the qualitative induction suggested by Bradley et al. (2).

ACKNOWLEDGMENTS

We thank Gabriel Di Mattia and Geoff Hicks for invaluable technical advice, Blair Gunhouse for transfection of pEJ lines, and Mike Mowat for critical evaluation of the work.

This work was supported by the National Cancer Institute of Canada, the Manitoba Health Research Council, and the Winnipeg Childrens' Hospital Research Foundation. S.E.E. is supported by a Steve Fonyo National Cancer Institute of Canada Studentship. A.H.G. and J.A.W. are Terry Fox Cancer Research Scientists.

LITERATURE CITED

1. **Bourne, H. R.** 1986. GTP-binding proteins: one molecular machine can transduce diverse signals. Nature (London) **321**:814–816.
2. **Bradley, M. O., A. R. Kraynak, R. D. Storer, and J. B. Gibbs.** 1986. Experimental metastasis in nude mice of NIH-3T3 cells containing various *ras* genes. Proc. Natl. Acad. Sci. USA **83**: 5277–5281.
3. **Chang, C.-C., J. E. Trosko, H.-J. Kung, D. Bonbick, and F. Matsumura.** 1985. Potential role of the *src* gene product in inhibition of gap-junction communication in NIH-3T3 cells. Proc. Natl. Acad. Sci. USA **82**:5360–5364.
4. **Chirgwin, J. M., A. E. Przbyla, R. J. McDonald, and W. J. Rutter.** 1979. Isolation of biologically active ribonucleic acid from sources enriched in ribonuclease. Biochemistry **18**: 5294–5299.
5. **Cifone, M. A., and I. J. Fidler.** 1980. Correlation of patterns of anchorage-independent growth with in vivo behavior of cells from a murine fibrosarcoma. Proc. Natl. Acad. Sci. USA **77**: 1039–1043.
6. **Ellis, R. W., D. DeFeo, M. E. Furth, and E. M. Scolnick.** 1982. Mouse cells contain two distinct *ras* gene mRNA species that can be translated into a p21 *onc* protein. Mol. Cell. Biol. **2**: 339–1345.
7. **Feinberg, A. P., and B. Vogelstein.** 1983. A technique for radiolabelling DNA restriction endonuclease fragments to high specific activity. Anal. Biochem. **132**:6–13.
8. **Feramisco, J. R., R. Clark, G. Wong, N. Arnheim, R. Milley, and F. McCormick.** 1985. Transient reversion of *ras* oncogene-induced cell transformation by antibodies specific for amino acid 12 of *ras* protein. Nature (London) **314**:639–642.
9. **Fidler, I. J., and M. L. Kripke.** 1977. Metastasis results from pre-existing variant cells within a malignant tumor. Science **197**:893–895.
10. **Fleischman, L. F., S. B. Chahwala, and L. Cantley.** 1986. *ras*-transformed cells: altered levels of phosphatidylinositol-4-5-bisphosphate and catabolites. Science **231**:407–410.
11. **Foulds, L.** 1975. Neoplastic development, vol. 2. Academic Press, Inc. (London), Ltd., London.
12. **Greig, R. G., T. P. Koestler, D. L. Trainer, S. P. Corwin, L. Miles, T. Kline, R. Sweet, S. Yokoyama, and G. Poste.** 1985. Tumorigenic and metastatic properties of "normal" and *ras*-transfected NIH/3T3 cells. Proc. Natl. Acad. Sci. USA **82**: 3698–3701.
13. **Huang, A. L., M. C. Ostrowski, D. Berard, and G. L. Hager.** 1981. Glucocorticoid regulation of the Ha-MuSV p21 gene conferred by sequences from mouse mammary tumor virus. Cell **27**:245–255.
14. **Kripke, M. L., E. Gruys, and I. J. Fidler.** 1978. Metastatic heterogeneity of cells from an ultraviolet light-induced murine fibrosarcoma of recent origin. Cancer Res. **38**:2962–2967.
15. **Land, H., L. F. Parada, and R. A. Weinberg.** 1983. Cellular oncogenes and multistep carcinogenesis. Science **222**:771–778.
16. **Lehrach, H., D. Diamond, J. W. Wozney, and H. Baldtker.** 1977. RNA molecular weight determinations by gel electrophoresis under denaturing conditions, a critical re-examination. Biochemistry **16**:4743–4751.
17. **Levinson, A. D.** 1986. Normal and activated *ras* oncogenes and

their encoded products. Trends Genet. **15**:81–85.
18. **Liotta, L. A.** 1986. Tumor invasion and metastasis—role of the extracellular matrix. Cancer Res. **46**:1–7.
19. **Maniatis, T., E. F. Fritsch, and J. Sambrook.** 1982. Molecular cloning: a laboratory manual. Cold Spring Harbor Laboratory, Cold Spring Harbor, N.Y.
20. **Martinet, Y., P. B. Bitterman, J.-F. Mornex, G. R. Grotendorst, G. R. Martin, and R. G. Crystal.** 1986. Activated human monocytes express the c-*sis* proto-oncogene and release a mediator showing PDGF-like activity. Nature (London) **319**: 158–160.
21. **Monoharan, T. H., J. A. Burgess, D. Ho, C. L. Newell, and W. E. Fahl.** 1985. Integration of a mutant c-Ha-*ras* oncogene into C3H/10T1/2 cells and its relationship to tumorigenic transformation. Carcinogenesis **6**:1295–1301.
22. **Mulcahy, L. S., M. R. Smith, and D. W. Stacey.** 1985. Requirement for *ras* proto-oncogene function during serum-stimulated growth of NIH-3T3 cells. Nature (London) **313**:241–243.
23. **Muschel, R. J., J. E. Williams, D. R. Lowy, and L. A. Liotta.** 1985. Harvey *ras* induction of metastatic potential depends upon oncogene activation and the type of recipient cell. Am J. Pathol. **121**:1–8.
24. **Nicolson, G. L.** 1982. Cancer metastasis: organ colonization and the cell-surface properties of malignant cells. Biochim. Biophys. Acta **695**:113–176.
25. **Nicolson, G. L., and G. Poste.** 1983. Tumor implantation and invasion at metastatic sites. Int. Rev. Exp. Pathol. **25**:77–181.
26. **Noda, M., M. Ko, A. Ogura, D. Liu, T. Amano, T. Takano, and Y. Ikawa.** 1985. Sarcoma viruses carrying *ras* oncogenes induce differentiation-associated properties in a neuronal cell line. Nature (London) **218**:73–75.
27. **Poste, G., and I. J. Fidler.** 1980. The pathogenesis of cancer metastasis. Nature (London) **283**:139–145.
28. **Pozzatti, R., R. Muschel, J. Williams, R. Padmanabhan, B. Howard, L. Liotta, and G. Khoury.** 1986. Primary rat embryo cells transformed by one or two oncogenes show different metastatic potentials. Science **232**:223–227.
29. **Pulciani, S., E. Santos, L. K. Long, V. Sorrentino, and M. Barbacid.** 1985. *ras* gene amplification and malignant transformation. Mol. Cell. Biol. **5**:2836–2841.
30. **Raaphorst, G. P., J. A. Vadasz, E. I. Azzam, M. D. Sargent, J. Borsa, and M. Einspenner.** 1985. Comparison of heat and/or radiation sensitivity and membrane composition of seven X-ray-transformed C3H 10T1/2 cell lines and normal C3H 10T1/2 cells. Cancer Res. **45**:5452–5456.
31. **Reed, K. C., and D. A. Mann.** 1985. Rapid transfer of DNA from agarose gels to nylon membranes. Nucleic Acids Res. **13**:7207–7221.
32. **Rigby, P. W., M. Dieckmann, C. Rhodes, and P. Berg.** 1977. Labeling deoxyribonucleic acid to high specific activity in vitro by nick-translation with DNA polymerase I. J. Mol. Biol. **113**:237–251.
33. **Rohrschneider, L., and S. Reynolds.** 1985. Regulation of cellular morphology by the Rous sarcoma virus *src* gene: analysis of fusiform mutants. Mol. Cell. Biol. **5**:3097–3107.
34. **Roos, E.** 1984. Cellular adhesion, invasion and metastasis. Biochim. Biophys. Acta **738**:263–284.
35. **Southern, E. M.** 1975. Detection of specific sequences among DNA fragments separated by gel electrophoresis. J. Mol. Biol. **98**:503–517.
36. **Stackpole, C. W., D. M. Fornabaio, and A. L. Alterman.** 1985. Phenotypic interconversion of B16 melanoma clonal cell populations: relationship between metastasis and tumor growth rate. Int. J. Cancer **35**:667–674.
37. **Thompson, C. B., P. B. Challoner, P. E. Neiman, and M. Groudine.** 1986. Expression of the c-*myb* proto-oncogene during cellular proliferation. Nature (London) **319**:374–380.
38. **Thorgeirsson, U. P., T. Turpeenniemi-Hujanen, J. E. Williams, E. H. Westin, C. A. Heilman, J. E. Talmadge, and L. A. Liotta.** 1985. NIH/3T3 cells transfected with human tumor DNA contianing activated *ras* oncogenes express the metastatic phenotype in nude mice. Mol. Cell. Biol. **5**:259–262.
39. **Vousden, K. H., S. A. Eccles, H. Purvies, and C. J. Marshall.** 1986. Enhanced spontaneous metastasis of mouse carcinoma cells transfected with an activated c-Ha-*ras*-1 gene. Int. J. Cancer **37**:425–433.
40. **Weissman, B., and S. A. Aaronson.** 1985. Members of the *src* and *ras* oncogene families supplant the epidermal growth factor requirement of BALB/MK-2 keratinocytes and induce distinct alterations in their terminal differentiation program. Mol. Cell. Biol. **5**:3386–3396.
41. **Wigler, M., S. Silverstein, L.-S. Lee, A. Pellicer, Y.-C. Cheng, and R. Axel.** 1977. Transfer of purified herpes virus thymidine kinase gene to cultured mouse cells. Cell **11**:223–232.
42. **Winter, E., and M. Perucho.** 1986. Oncogene amplification during tumorigenesis of established rat fibroblasts reversibly transformed by activated human *ras* oncogenes. Mol. Cell. Biol. **6**:2562–2570.